

Drastic Enhancement of the CO₂ Adsorption Properties in Sulfone-Functionalized Zr- and Hf-UiO-67 MOFs with Hierarchical Mesopores

Pantelis Xydias, Ioannis Spanopoulos, Emmanuel Klontzas, George E. Froudakis, and Pantelis N. Trikalitis*

Department of Chemistry, University of Crete, Voutes 71003, Heraklion, Greece

S Supporting Information

ABSTRACT: The sulfone-functionalized Zr- and Hf-UiO-67 metal–organic frameworks with hierarchical mesopores were successfully synthesized using the ligand 4,4'-dibenzoic acid-2,2'-sulfone, with acetic acid or HCl as the modulator. Compared to UiO-67, the zirconium solid shows a remarkable 122% increase in CO₂ uptake, reaching 4.8 mmol g⁻¹ (17.4 wt %) at 1 bar and 273 K (145% at 298 K) and more than 100% increase in CO₂/CH₄ selectivity.

Currently, an enormous research activity is devoted to porous metal–organic frameworks (MOFs) or porous coordination polymers mainly because of the prospect of finding application in important technological sectors related to energy and the environment.¹ In particular, the reduction of greenhouse gas emissions and especially CO₂ is currently a major target worldwide, and highly porous sorbents like MOFs hold great promise as cost-effective alternatives to the existing technologies.^{1b,2,3}

A particular MOF that has captured a great deal of attention because of its high thermal and chemical stability is the zirconium-based, 12-connected Zr₆(μ₃-O)₄(μ₃-OH)₄(bdc)₆ (UiO-66) microporous material, made with terephthalate dianions (bdc²⁻).⁴ This material shows interesting CO₂ sorption properties especially for low-pressure and ambient-temperature applications that can be further improved with functionalized H₂bdc linkers⁵ and, in particular, with those containing the highly polar sulfonic acid group, as has been demonstrated both theoretically^{5b} and experimentally.^{5c} The isostructural analogue UiO-67, based on the linker 4,4'-biphenyldicarboxylate (bpdcc²⁻), because of its larger pore size and increased pore volume, is considered as a very promising material for CO₂ adsorption.⁶ However, related studies are limited,⁷ and to the best of our knowledge, there is no report on functionalized UiO-67.

We report here the synthesis and characterization of the sulfone-functionalized analogue of UiO-67(Zr), using the ligand 4,4'-dibenzoic acid-2,2'-sulfone (H₂bbs), in the presence of acetic acid (AcOH) or HCl as the modulator, denoted as **1**_{AcOH} and **1**_{HCl}, respectively. We have also isolated the hafnium analogues, denoted as **2**_{AcOH} and **2**_{HCl}. For comparison purposes, we synthesized Zr-UiO-67 using the ligand 4,4'-biphenyldicarboxylic acid (H₂bpdcc), denoted as **3**_{AcOH} and **3**_{HCl}. Remarkably, compared to the parent, high-quality nonfunctionalized solid **3**_{AcOH}, **1**_{AcOH} shows a 122% increase in CO₂ uptake at 1 bar and

273 K (145% at 298 K), reaching 4.8 mmol g⁻¹ (2.88 mmol g⁻¹ at 298 K), with high selectivity toward CH₄ and N₂. In terms of key structural features, we provide a direct proof, using ¹H NMR spectroscopy, for the presence of AcO⁻ anions coordinated to the Zr₆ clusters in **1**_{AcOH}. Moreover, both AcOH and HCl induce in **1**_{AcOH} and **1**_{HCl} hierarchical mesopores. Below, we present and discuss a detailed structural and gas sorption study of the zirconium-based solids, although key findings for the hafnium analogues are also reported.

Because of the lack of suitable single crystals, the ideal structure of **1** shown in Figure S2 was built using a ligand replacement methodology starting from the known structure of UiO-66.⁴ The powder X-ray diffraction (PXRD) patterns of high-quality **1**_{AcOH} and **2**_{AcOH} are shown in Figure 1. All

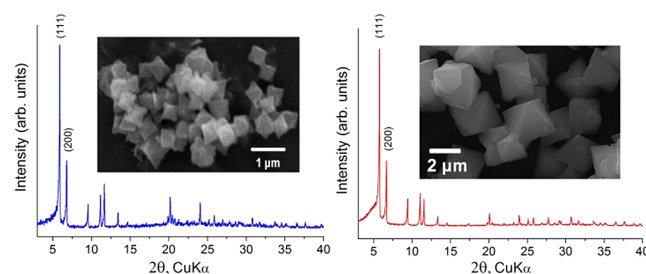


Figure 1. Powder X-ray diffraction pattern of **1**_{AcOH} (left) and **2**_{AcOH} (right). Insets: representative SEM images.

compounds are isostructural, and the PXRD pattern can be indexed to the cubic system with refined unit cells of 26.61(2), 26.54(3), and 26.87(2) Å for **1**_{AcOH}, **2**_{AcOH}, and **3**_{HCl}, respectively. The smaller unit cell of **1**_{AcOH} and **2**_{AcOH} compared to **3**_{HCl} is due to the shorter length of the bbs²⁻ linker caused by the bending of the two aromatic rings. It is worth noticing that, despite its large deviation from linearity (163°), this linker is capable of forming an isostructural solid with UiO-67.

Argon sorption isotherms at 87 K for **1**_{AcOH}, **1**_{HCl}, and **3**_{HCl} are shown in Figure 2, from which important porosity data were determined and are summarized in Table S1 in the Supporting Information (SI). Accordingly, both **1**_{AcOH} and **1**_{HCl} show almost identical Brunauer–Emmett–Teller (BET) areas, 1442 m² g⁻¹ (Langmuir 1597 m² g⁻¹) and 1456 m² g⁻¹ (Langmuir 1601 m² g⁻¹), respectively, which are lower compared to **3**_{HCl} (BET area 1996 m² g⁻¹ and Langmuir 2253 m² g⁻¹) presumably because of

Received: September 25, 2013

Published: December 24, 2013

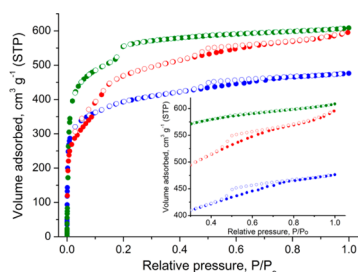


Figure 2. Argon adsorption (closed circles) and desorption (open circles) isotherms at 87 K of 1_{AcOH} (blue), 1_{HCl} (red), and 3_{HCl} (green). Inset: hysteresis in 1_{AcOH} and 1_{HCl} .

the presence of the sulfone groups. The PXRD patterns of the activated samples 1_{AcOH} , 2_{AcOH} , 3_{HCl} , and 3_{AcOH} are identical with those of the as-made materials, while notably for the corresponding 1_{HCl} and 2_{HCl} , a significantly reduced crystallinity is observed (see the SI). We found that the functionalized solids and especially the evacuated materials, compared to UiO-67, show enhanced moisture sensitivity (evacuated solids stored in dry conditions are stable for months), and this is attributed to the presence of the polar sulfone groups that make the solids more hydrophilic. The degradation mechanism of the $\text{Zr}_6\text{O}_4(\text{OH})_4$ cluster by water in UiO-type solids has been reported recently.⁸ ^1H NMR measurements of acid-digested, activated samples confirm the complete removal of solvent molecules. Moreover, the ^1H NMR spectrum of 1_{AcOH} shows the presence of AcOH in a 1:2.5 ratio with H_2bbs . This ratio is reproducible in different batches of activated 1_{AcOH} . Furthermore, energy-dispersive spectroscopy (EDS) shows the absence of Cl^- anions. These results suggest that the observed AcOH originates from AcO^- anions coordinated to the Zr_6 clusters at the expense of bridging bbs^{2-} linkers. Accordingly, the proposed charge-balanced chemical formula of the activated 1_{AcOH} is $\text{Zr}_6(\mu_3\text{-O})_4(\mu_3\text{-OH})_4(\text{bbs})_5(\text{AcO})_2$. This formula is also supported by thermogravimetric analysis (TGA); see the SI. Although in UiO-66 solids it has been recognized that the Zr_6 clusters can be defective, in its AcOH-modulated synthesis, the presence of a coordinated AcO^- ligand was confirmed by neutron inelastic scattering experiments very recently, however without quantitative results.⁹ In a more recent report, the presence of coordinated trifluoroacetate anions in UiO-66 was confirmed by solid-state ^{19}F NMR spectroscopy.¹⁰ Interestingly, the observed Zr_6 to bdc^{2-} ratio was 4.

The large amount of stoichiometric defects in 1_{AcOH} , due to the presence of coordinated AcO^- ligands, is expected to create hierarchical mesoporosity. Indeed, accurate pore-size analysis from the argon isotherm of 1_{AcOH} confirmed the presence of mesopores, as we discuss below. The presence of a small hysteresis step during desorption at $P/P_0 \sim 0.5$ is in agreement with the existence of mesopores (see the inset in Figure 2). Notably, very similar types of isotherms were observed in MOFs with functionalized mesopores using a metal–ligand–fragment coassembly strategy,¹¹ which, in fact, resembles the synthesis of 1_{AcOH} . Our findings are consistent with a recent report on the formation of mesopores in UiO-66 due to missing linker defects.^{9b}

High-resolution micropore analysis of 1_{AcOH} using argon at 87 K (see Figure S13 in the SI) allowed us to calculate the corresponding pore-size distribution using nonlocal density functional theory (NLDFT). Accordingly, two distinct peaks centered at 6.3 and 8.4 Å are observed, in agreement with the

expected size of the microporous tetrahedral and octahedral cages in 1_{AcOH} (see Figure S14 in the SI). In addition, two relatively narrow peaks and one broad, centered at 15, 25, and 50 Å, respectively, are observed, consistent with the presence of hierarchical mesopores.

For comparison purposes, we first synthesized and studied the properties of an HCl-modulated UiO-67 (3_{HCl}) because it is reported to be stable.⁶ The corresponding porosity data are summarized in Table S1 in the SI. The argon adsorption isotherm of 3_{HCl} in addition to the microporous knee at low relative pressures ($P/P_0 < 0.1$), shows a well-defined condensation step at $P/P_0 \sim 0.2$, suggesting the presence of uniform, small mesopores. The corresponding NLDFT analysis revealed three distinct peaks centered at 6.4, 9.5, and 27.2 Å (see Figure S34 in the SI). While the first two peaks are expected from the crystal structure (tetrahedral and octahedral cages), the narrow mesoporous peak at 27.2 Å is observed for the first time in the UiO-67 literature.^{4,6,12} Taking into account that no Cl^- anions are observed in EDS, TGA suggests the presence of defects, presumably in the form of $-\text{OH}$ groups coordinated to the Zr_6 clusters. The indicated charge-balanced chemical formula is $\text{Zr}_6(\mu_3\text{-O})_4(\mu_3\text{-OH})_4(\text{bpc})_{4.7}(\text{OH})_{2.6}$. Notably, in the HCl-modulated synthesis of UiO-66,¹⁰ the Zr_6 : bdc ratio is 5. On the basis of these results, the formation of uniform mesopores in 3_{HCl} is attributed to the large amount of HCl used for its synthesis. Compared to the reported pure microporous UiO-67 made with 2 equiv of HCl, 3_{HCl} was made with 35. To verify our proposition, we synthesized 1_{HCl} with a similar large excess of HCl. Indeed, the argon adsorption isotherm at 87 K of 1_{HCl} shows a clear condensation step at $P/P_0 \sim 0.1$ consistent with the presence of uniform small mesopores, however larger in size than those in 1_{AcOH} , resulting in an increased total pore volume (see Table S1 in the SI). The observed larger pore size is attributed to the absence of bulky coordinated AcO^- anions in 1_{HCl} and to additional structural defects because of its reduced quality, as judged by scanning electron microscopy (SEM). Accordingly, 1_{AcOH} consists of uniform particles in single-crystal form (see Figure 1), while highly irregular particles are observed in 1_{HCl} . This is also the case between $2_{\text{AcOH}}/2_{\text{HCl}}$ and $3_{\text{AcOH}}/3_{\text{HCl}}$ (see Figure 1 and the SI), indicating the important role of AcOH in slowing down the reaction kinetics, leading to the formation of uniform well-shaped particles, in agreement with the literature results.¹²

The CO_2 , CH_4 , N_2 , and H_2 sorption properties were investigated at different temperatures and pressures from which the uptake, isosteric heat of adsorption (Q_{st}), and selectivity using IAST were calculated and are discussed below (see the SI). Figure 3 shows the low-pressure CO_2 adsorption isotherms for 1_{AcOH} and 3_{AcOH} (3_{HCl} performs almost

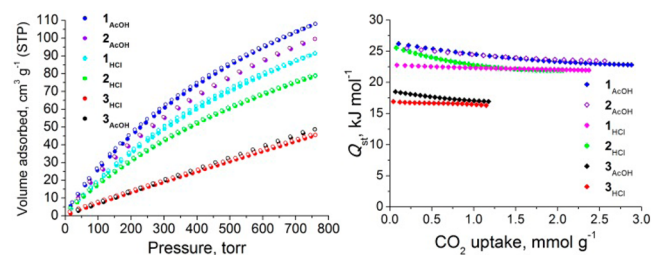


Figure 3. CO_2 adsorption (closed symbols)/desorption (open symbols) isotherms for the indicated solids at 273 K (left) and the corresponding heats of adsorption (right).

identically), at 273 K up to 1 bar. Remarkably, under these conditions, I_{AcOH} shows a 122% (145% at 298 K) increase in CO_2 uptake compared to 3_{AcOH} , reaching 4.84 mmol g^{-1} , despite its significantly lower BET area (see Table S1 in the SI). This uptake is 20% higher compared to the titanium-substituted Zr-UiO-66^{13a} (4.0 mmol g^{-1}) and among the highest reported in the entire family of UiO-type solids,^{13b} under the same experimental conditions. At 273 K and 20 bar, the CO_2 uptake of I_{AcOH} is 13.3 mmol g^{-1} , while at 195 K and 1 bar, it is 16.5 mmol g^{-1} (see the SI). With an identical BET area, I_{HCl} at 273 K and 1 bar adsorbs 4.0 mmol g^{-1} . In comparison to I_{AcOH} , the 17% decrease in CO_2 uptake is related to the reduced number of bbs^{2-} linkers (less sulfone groups) per Zr_6 cluster in I_{HCl} (4.7 versus 5) and also to the increased pore size (reduced attracting potential). In line with that above, the heavier hafnium analogues, 2_{HCl} and 2_{AcOH} , adsorb 3.5 and 4.5 mmol g^{-1} of CO_2 at 273 K and 1 bar, respectively (see Table S1 in the SI and Figure 3).

The calculated Q_{st} values at zero coverage (Q_{st}°) using the adsorption data at 273 and 298 K are 26.5 and 18.5 kJ mol^{-1} for I_{AcOH} and 3_{AcOH} (16.9 kJ mol^{-1} for 3_{HCl}), respectively. As a function of the surface coverage, Q_{st} is slightly decreasing for I_{AcOH} , reaching 22.9 kJ mol^{-1} at high coverage (see Figure 3). These medium-ranged Q_{st} values are considered promising for low-cost regeneration of porous CO_2 adsorbers.^{1b,2b,3} The substantial increase of 8 kJ mol^{-1} in Q_{st}° between I_{AcOH} and 3_{AcOH} is attributed mainly to the polar sulfone groups that interact stronger with CO_2 because of its quadrupole moment.^{1b} Accurate ab initio calculations show that, in going from the H_2bpdC to the H_2bbs linker, the increase in the CO_2 binding strength is approximately 30% (3.2 and $4.1 \text{ kcal mol}^{-1}$, respectively). However, for the observed increase in the CO_2 uptake (145% at 298 K) and 55% in Q_{st} , additional factors are contributing, including a decrease in the pore size, which increases the overlap of attractive potential fields of opposite surfaces, leading to stronger and higher CO_2 adsorption.

Regarding CH_4 , Q_{st}° values for I_{AcOH} and 3_{HCl} are 14.5 and 8.9 kJ mol^{-1} , respectively. The CO_2/CH_4 selectivity in I_{AcOH} at 273 K/298 K using IAST for a 5/95 molar mixture is 9.8/6.8, while for 3_{HCl} , it is significantly lower, 4.0/3.2 (see the SI). The observed more than 100% increase in selectivity is attributed to the increased interaction of CO_2 with the polar sulfone groups. The CO_2/N_2 selectivity in I_{AcOH} at 273 K/298 K is 23.9/24.5. The CO_2/CH_4 and CO_2/N_2 selectivities in I_{AcOH} are among the highest for MOFs without open metal sites or amine groups.^{1b} Finally, the H_2 uptake at 77 K is 25% higher in I_{AcOH} (1.5 wt %) compared to 3_{HCl} (1.2 wt %), with Q_{st}° values of 7.4 and 6.3 kJ mol^{-1} , respectively.

In conclusion, we have shown that the insertion of polar sulfone groups into UiO-67 increases drastically the CO_2 uptake and selectivity. Control over missing linker defects using AcOH and HCl or other types of modulators offers the possibility of preparing materials with adjustable hierarchical mesoporosity. In addition, given the available organic linkers that can be functionalized with sulfone groups, our findings could be utilized to prepare a family of new zirconium-based MOFs with improved CO_2 adsorption properties.

■ ASSOCIATED CONTENT

■ Supporting Information

Experimental procedures, gas sorption isotherms and related calculations, IR, NMR, TGA, and SEM/EDS. This material is available free of charge via the Internet at <http://pubs.acs.org>.

■ AUTHOR INFORMATION

Corresponding Author

*E-mail: ptrikal@chemistry.uoc.gr.

Notes

The authors declare no competing financial interest.

■ ACKNOWLEDGMENTS

This work was supported by the “Heracleitus II” and “THALES” programs funded by GSRT in Greece.

■ REFERENCES

- (1) (a) Suh, M. P.; Park, H. J.; Prasad, T. K.; Lim, D.-W. *Chem. Rev.* **2012**, *112*, 782–835. (b) Sumida, K.; Rogow, D. L.; Mason, J. A.; McDonald, T. M.; Bloch, E. D.; Herm, Z. R.; Bae, T.-H.; Long, J. R. *Chem. Rev.* **2012**, *112*, 724–781. (c) Makal, T. A.; Li, J. R.; Lu, W. G.; Zhou, H. C. *Chem. Soc. Rev.* **2012**, *41*, 7761–7779.
- (2) (a) Markewitz, P.; Kuckshinrichs, W.; Leitner, W.; Linssen, J.; Zapp, P.; Bongartz, R.; Schreiber, A.; Muller, T. E. *Energy Environ. Sci.* **2012**, *5*, 7281–7305. (b) Li, J. R.; Ma, Y. G.; McCarthy, M. C.; Sculley, J.; Yu, J. M.; Jeong, H. K.; Balbuena, P. B.; Zhou, H. C. *Coord. Chem. Rev.* **2011**, *255*, 1791–1840.
- (3) (a) Nugent, P.; Belmabkhout, Y.; Burd, S. D.; Cairns, A. J.; Luebke, R.; Forrest, K.; Pham, T.; Ma, S. Q.; Space, B.; Wojtas, L.; Eddaoudi, M.; Zaworotko, M. J. *Nature* **2013**, *495*, 80–84. (b) Xue, D. X.; Cairns, A. J.; Belmabkhout, Y.; Wojtas, L.; Liu, Y.; Alkordi, M. H.; Eddaoudi, M. J. *Am. Chem. Soc.* **2013**, *135*, 7660–7667.
- (4) Cavka, J. H.; Jakobsen, S.; Olsbye, U.; Guillou, N.; Lamberti, C.; Bordiga, S.; Lillerud, K. P. *J. Am. Chem. Soc.* **2008**, *130*, 13850–13851.
- (5) (a) Biswas, S.; Van der Voort, P. *Eur. J. Inorg. Chem.* **2013**, 2154–2160. (b) Yang, Q. Y.; Wiersum, A. D.; Llewellyn, P. L.; Guillerm, V.; Serred, C.; Maurin, G. *Chem. Commun.* **2011**, *47*, 9603–9605. (c) Biswas, S.; Zhang, J.; Li, Z. B.; Liu, Y. Y.; Grzywa, M.; Sun, L. X.; Volkmer, D.; Van der Voort, P. *Dalton Trans.* **2013**, *42*, 4730–4737. (d) Jasuja, H.; Zang, J.; Sholl, D. S.; Walton, K. S. *J. Phys. Chem. C* **2012**, *116*, 23526–23532. (e) Foo, M. L.; Horike, S.; Fukushima, T.; Hijikata, Y.; Kubota, Y.; Takata, M.; Kitagawa, S. *Dalton Trans.* **2012**, *41*, 13791–13794. (f) Kim, M.; Cohen, S. M. *CrystEngComm* **2012**, *14*, 4096–4104. (g) Abid, H. R.; Ang, H. M.; Wang, S. B. *Nanoscale* **2012**, *4*, 3089–3094.
- (6) Yang, Q. Y.; Guillerm, V.; Ragon, F.; Wiersum, A. D.; Llewellyn, P. L.; Zhong, C. L.; Devic, T.; Serre, C.; Maurin, G. *Chem. Commun.* **2012**, *48*, 9831–9833.
- (7) Nik, O.; Chen, X. Y.; Kaliaguine, S. *J. Membr. Sci.* **2012**, *413*, 48–61.
- (8) DeCoste, J. B.; Peterson, G. W.; Jasuja, H.; Glover, T. G.; Huang, Y. G.; Walton, K. S. *J. Mater. Chem. A* **2013**, *1*, 5642–5650.
- (9) (a) Valenzano, L.; Civalleri, B.; Chavan, S.; Bordiga, S.; Nilsen, M. H.; Jakobsen, S.; Lillerud, K. P.; Lamberti, C. *Chem. Mater.* **2011**, *23*, 1700–1718. (b) Wu, H.; Chua, Y. S.; Krungleviciute, V.; Tyagi, M.; Chen, P.; Yildirim, T.; Zhou, W. *J. Am. Chem. Soc.* **2013**, *135*, 10525–10532.
- (10) Vermeortele, F.; Bueken, B.; Le Bars, G. L.; Van de Voorde, B.; Vandichel, M.; Houthoofd, K.; Vimont, A.; Daturi, M.; Waroquier, M.; Van Speybroeck, V.; Kirschhock, C.; De Vos, D. E. *J. Am. Chem. Soc.* **2013**, *135*, 11465–11468.
- (11) Park, J.; Wang, Z. Y. U.; Sun, L. B.; Chen, Y. P.; Zhou, H. C. *J. Am. Chem. Soc.* **2012**, *134*, 20110–20116.
- (12) Schaate, A.; Roy, P.; Godt, A.; Lippke, J.; Waltz, F.; Wiebcke, M.; Behrens, P. *Chem.—Eur. J.* **2011**, *17*, 6643–6651.
- (13) (a) Lau, C. H.; Babarao, R.; Hill, M. R. *Chem. Commun.* **2013**, *49*, 3634–3636. (b) Jiang, H. L.; Feng, D. W.; Liu, T. F.; Li, J. R.; Zhou, H. C. *J. Am. Chem. Soc.* **2012**, *134*, 14690–14693.